

# Giant Isotope Effect in the Incoherent Tunneling Specific Heat of the Molecular Nanomagnet $\text{Fe}_8$

M. Evangelisti<sup>1,2</sup>, F. Luis<sup>3</sup>, F. L. Mettes<sup>1</sup>, R. Sessoli<sup>4</sup>, and L. J. de Jongh<sup>1</sup>

<sup>1</sup> *Kamerlingh Onnes Laboratory, Leiden University, 2300 RA Leiden, The Netherlands*

<sup>2</sup> *National Research Center on “nanoStructures and bioSystems at Surfaces” (S<sup>3</sup>), INFN-CNR, 41100 Modena, Italy*

<sup>3</sup> *Instituto de Ciencia de Materiales de Aragón,*

*CSIC-Universidad de Zaragoza, 50009 Zaragoza, Spain*

<sup>4</sup> *Dipartimento di Chimica, Università di Firenze, 50144 Firenze, Italy*

(Dated: May 16, 2018)

Time-dependent specific heat experiments on the molecular nanomagnet  $\text{Fe}_8$  and the isotopic enriched analogue  $^{57}\text{Fe}_8$  are presented. The inclusion of the  $^{57}\text{Fe}$  nuclear spins leads to a huge enhancement of the specific heat below 1 K, ascribed to a strong increase in the spin-lattice relaxation rate  $\Gamma$  arising from incoherent, nuclear-spin-mediated magnetic quantum tunneling (MQT) in the ground-doublet. Since  $\Gamma$  is found comparable to the expected tunneling rate, the MQT process has to be inelastic. A model for the coupling of the tunneling spins to the lattice is presented. Under transverse field, a crossover from nuclear-spin-mediated to phonon-induced tunneling is observed.

PACS numbers: 75.40.-s, 75.45.+j, 75.50.Xx

Single-molecule magnets are fascinating nano-size superparamagnetic particles which at low temperatures may flip their magnetic moments by magnetic quantum tunneling (MQT) through the anisotropy barrier [1]. Observation of quantum tunneling in these molecules illustrates the complexity of the interaction of such magnetic qubits with their “environment” (neighboring particles, nuclear spins, phonons). Indeed, the tunnel splitting  $\Delta$  of the magnetic ground-state is many orders of magnitude smaller than the energy bias  $\xi$  from, e.g., dipolar interactions between molecules, rendering MQT impossible at first sight. It is by now well established, both theoretically [2, 3] and experimentally [4, 5, 6], that *incoherent* MQT is yet possible through the presence of rapidly fluctuating nuclear spins. The resulting dynamical hyperfine bias may, at any time, bring a fraction of the molecular spins into resonance, thus opening an energy window  $E_w \gg \Delta$  for incoherent tunneling.

It should be emphasized that in the Prokof'ev/Stamp (PS) model [2], relaxation of the magnetic moment of the molecular cluster (hereafter, cluster spin) is to the nuclear spin bath. A coupling to the lattice is not considered, the argument being [7] that only at long times relaxation by phonons will become more efficient than the nuclear-spin-mediated magnetic relaxation. However, time-dependent specific heat experiments [6, 8] neatly show that (for high enough MQT rate) both the electronic and nuclear spin systems can remain in thermal equilibrium with the lattice even deep into the quantum regime, where the only fluctuations possible are those arising from MQT events. This strongly suggests that, whereas the nuclear spins are needed to relax the (otherwise blocked) electron spins through MQT, at the same time the MQT mechanism apparently enables relaxation of both nuclear and electron spins to the lattice. Interestingly, in magnetic insulating compounds such as these,

relaxation of nuclear spins to the lattice has to occur via the electron spin-phonon channel, direct nuclear relaxation to the lattice being extremely slow at low temperatures. In other words, by enabling the cluster spins to tunnel, the nuclei themselves can relax to the lattice!

In this Letter we present definite proof for this unusual scenario. By comparing the low- $T$  specific heat arising from incoherent tunneling in the ground-doublet for  $\text{Fe}_8$  and its  $^{57}\text{Fe}$ -enriched counterpart  $^{57}\text{Fe}_8$ , we show that the inclusion of the  $^{57}\text{Fe}$  nuclear moments in the (otherwise identical) molecules leads to an enormous enhancement of the specific heat below 1 K, which can only result from a strong increase in the spin-lattice relaxation rate  $\Gamma$ . Below 1 K, this rate is found to be several orders of magnitude larger than predicted for conventional spin-lattice relaxation [9]. To explain our results an extension of the PS model is presented that includes inelastic tunneling events, in which a spin-flip is accompanied by the creation or annihilation of low-energy phonons.

Low-temperature ( $0.1 \text{ K} < T < 7 \text{ K}$ ) specific heat  $C$  measurements were performed in a home-made calorimeter [6] using the thermal relaxation method. By varying the thermal resistance of the link between calorimeter and cold-sink, the characteristic timescale  $\tau_e$  of the experiment can be varied. In this way measurements of the time-dependent  $C$  can be exploited to probe the long-time ( $0.1 - 10^2 \text{ s}$ ) magnetic relaxation [6]. At higher temperatures ( $T > 2 \text{ K}$ ),  $C$  was measured using a commercial calorimeter. The enriched sample, denoted by  $^{57}\text{Fe}_8$ , was prepared as described in Ref. [5]. Except for the presence of the  $^{57}\text{Fe}$  nuclear moments in  $^{57}\text{Fe}_8$  (enriched to 95% in  $^{57}\text{Fe}$ ), no difference in the magnetic structure between  $\text{Fe}_8$  and  $^{57}\text{Fe}_8$  is to be expected.

We first discuss the zero-field specific heat data. In Fig. 1, we compare the specific heat  $C/R$  of a non-oriented powder  $^{57}\text{Fe}_8$  sample, as measured with two dif-

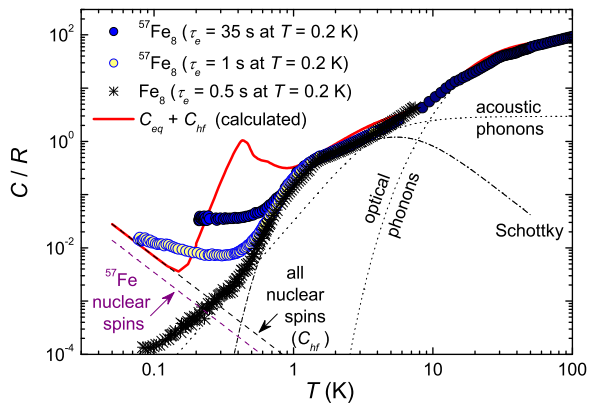


FIG. 1: (color online) Zero-field specific heats of non-oriented samples of standard  $\text{Fe}_8$  and of  $^{57}\text{Fe}_8$  as a function of temperature. For  $^{57}\text{Fe}_8$ , data for  $\tau_e \approx 35$  s ( $\bullet$ ) and 1 s ( $\circ$ ) are given, whereas for  $\text{Fe}_8$ ,  $\tau_e \approx 0.5$  s ( $*$ ). Drawn curves are explained in the text.

ferent thermal links, with our previous data [6] on non-oriented  $\text{Fe}_8$ . The specific heat contains contributions from the phonon modes of the crystal lattice as well as magnetic contributions from electronic and nuclear spins. The lattice specific heat can be described by the sum of a Debye curve, which describes the contribution of acoustic phonon modes, plus an Einstein oscillator term that probably arises from intramolecular vibrational modes (optical phonons). The overall fit yields for both samples  $\theta_D \simeq 19$  K and  $\theta_E \simeq 38$  K for the Debye and Einstein temperatures, respectively [10], (plotted in Fig. 1 as dotted curves).

Above 1 K, the magnetic contribution  $C_m$  to the specific heat of both compounds is independent of  $\tau_e$ . In this range, the equilibrium  $C_m$  mainly arises from transitions between the energy levels of the molecular spin  $S = 10$ , split by the uniaxial anisotropy [6, 11]. The associated multilevel Schottky anomaly  $C_0$  is shown as the dash/dotted curve in Fig. 1. Below 1 K, the remaining entropy arises almost completely from the ground-state doublet  $\pm 10$ , which is split by intercluster magnetic dipolar couplings and by hyperfine interactions between the electronic and nuclear spins. Dipolar interactions can induce, under equilibrium conditions, a long-range ordered magnetic phase. In Fig. 1, we plot the equilibrium specific heat  $C_{eq}$  of  $\text{Fe}_8$ , obtained from Monte-Carlo calculations [12], which predicts the occurrence of such a phase transition at  $T_C \simeq 0.43$  K. However, the equilibration of the relative populations of the two lowest levels, either by thermal activation or by tunneling, is a very slow process [11], thus  $C_m$  measured at finite  $\tau_e$  does not reach its equilibrium value. Indeed, as shown in Fig. 1 (see also [6]), the specific heat deviates from equilibrium below a blocking temperature  $T_B \simeq 1.2$  K, indicating

that the electronic spin-lattice relaxation rate  $\Gamma$  becomes smaller than  $\tau_e^{-1}$ .

In this non-equilibrium regime we observe a spectacular isotope effect. For the standard  $\text{Fe}_8$ ,  $C_m \sim C_0$  below  $T \sim 1$  K, decreasing exponentially to nearly zero (below  $\sim 0.4$  K the measured  $C$  basically equals the Debye term). By contrast,  $C_m$  of  $^{57}\text{Fe}_8$  is about 100 times larger and it increases with  $\tau_e$ . We mention here that  $\tau_e$  varies weakly with  $T$  and is determined for each data point. The  $\tau_e$  values mentioned in Figs. 1 and 2 are those estimated at  $T = 0.2$  K for each particular  $T$ -sweep. The strong isotope effect is a direct evidence that  $\Gamma$ , i.e. the thermal contact between the lattice and electronic spin systems, is enhanced as a result of the introduction of  $^{57}\text{Fe}$  nuclear spins. Although the rate is not yet sufficient to ensure complete thermal equilibrium within the experimental time constants available, a sizable part of the entropy of the ground-doublet is now removed.

It should be added that the  $^{57}\text{Fe}$  nuclear spins  $I = 1/2$  will also contribute to the zero-field  $C/R$ . In thermal equilibrium, this contribution amounts to  $C_{hf}(^{57}\text{Fe})/R = A^2 s^2 I(I+1)/3(k_B T)^2$ , where  $A$  is the hyperfine coupling and  $s = 5/2$  is the  $\text{Fe}^{3+}$  electronic spin. Taking  $A/k_B = 1.65$  mK estimated by Stamp and Tupitsyn [13], we obtain the  $T^{-2}$ -term indicated by the lower dashed curve in Fig. 1. The higher dashed curve in Fig. 1 gives the equilibrium nuclear  $C_{hf}$  calculated by adding the contributions of nuclear spins at the 120 protons, the 18  $^{14}\text{N}$  nuclei and the 8  $^{79,81}\text{Br}$  nuclei present in the  $\text{Fe}_8$  molecule. Note that at  $T \approx 0.2$  K,  $C_{hf}$  is one to two orders of magnitude smaller than the measured  $C$  for  $^{57}\text{Fe}_8$ . Further, see for standard  $\text{Fe}_8$  that  $C$  becomes smaller than  $C_{hf}$  at  $T \approx 0.1$  K, suggesting that also nuclear spins are off equilibrium.

We next discuss experiments performed under applied magnetic field. Figure 2 shows results for  $^{57}\text{Fe}_8$  measured at  $T \simeq 0.22$  K, compared to previous data for  $\text{Fe}_8$  obtained for nearly the same  $T$  and  $\tau_e$  [6]. At such high- $B$  and low- $T$ ,  $C_m$  of a randomly oriented sample is dominated by the contribution of those crystals whose anisotropy axes lie nearly perpendicular to the field. To substantiate this statement, we calculated that, at  $T = 0.2$  K and  $B = 1.5$  T, those crystals making an angle smaller than  $87.5^\circ$  with the field contribute less than one percent to the electronic equilibrium  $C$ . These experiments give thus information on the way the spin-lattice relaxation is modified by  $B_\perp$ .

In agreement with the zero-field-behavior, the  $C_m$  curves of the two isotopic derivatives are very different for  $B < 1.5$  T (Fig. 2). For higher fields, however, they are seen to merge within the experimental uncertainties. The observed dependence on the applied field can be well explained in terms of a tunable quantum tunneling rate. The perpendicular field introduces off-diagonal terms in the spin Hamiltonian, which increase the tunnel splitting  $\Delta$  by many orders of magnitude. When  $\Delta$  becomes

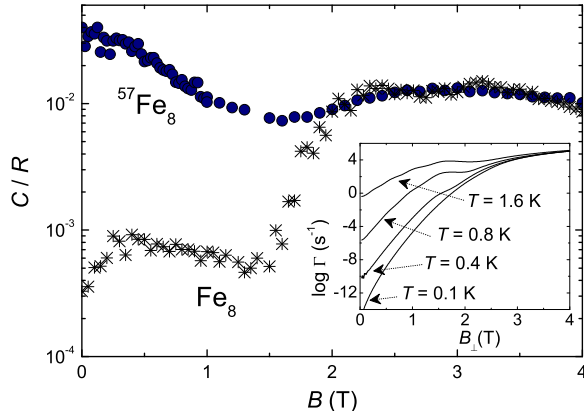


FIG. 2: (color online) Field-dependence of the specific heat of  $^{57}\text{Fe}_8$  measured at  $T = 0.22$  K, (for  $\tau_e \approx 35$  s), together with previous data [6] obtained for  $\text{Fe}_8$  at 0.24 K. Inset: Calculated  $\Gamma(B_\perp)$  associated with ‘conventional’ direct processes (see text) for several  $T$ .

larger than  $E_w$ , the tunneling rate becomes no longer determined by the hyperfine interactions but rather by  $\Delta$ . Then  $\Gamma$  should become nearly the same for both compounds, as observed. Besides phonon-assisted tunneling, the increase of  $\Delta$  also leads to strong enhancement of the relaxation rate associated with ‘conventional’ direct processes of emission and absorption of phonons. This is shown in the inset of Fig. 2, where we plot  $\Gamma(B_\perp)$  calculated [14] using the anisotropy parameters from Ref. [15]. For  $B_\perp \gtrsim 2.2$  T,  $\Gamma$  becomes of the same order of the experimental  $\tau_e^{-1}$ . This explains why conventional theory for spin-lattice relaxation accounts quantitatively for the transition to equilibrium observed at large transverse fields [6], although it completely fails to account for the zero field data.

To obtain quantitative information on the rate at which the spins approach thermal equilibrium at low  $T$  in zero field, we need to assume a particular expression for the time-dependence of  $C_m$ . This is complicated by the fact that, at low  $T$  and especially below the ordering temperature  $T_C$ , relaxation to equilibrium becomes a collective process in which each spin-flip modifies the dipolar biases acting on the other spins [2]. This problem was theoretically studied by Fernández [16], who calculated numerically the time-dependent  $C_m$  of a lattice of *interacting* Ising spins flipping by quantum tunneling. Within this model,  $C_m \simeq C_0 + (\tilde{c} T_C^2/T)(\Gamma/v)$  where  $v \equiv dT/dt$  is the temperature sweeping-rate and  $\tilde{c}$  is a constant that depends on the symmetry and lattice parameters. In our experiments,  $v \simeq \Delta T/\tau_e$ , where  $\Delta T \simeq 0.05 T$  is the  $T$ -change of the calorimeter in each data point. It is therefore possible to determine  $\Gamma$ , up to a constant factor, from  $C_m$ . Moreover, above  $T_C$  we can also fit  $C_m$  assuming a simple exponential de-

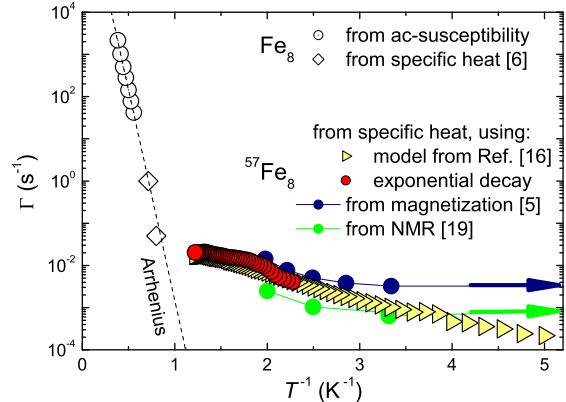


FIG. 3: (color online) Spin-lattice relaxation rates of standard  $\text{Fe}_8$  and  $^{57}\text{Fe}_8$  obtained by different experimental techniques, as labelled. Dashed curve is the Arrhenius fit to the high- $T$  data. Arrows indicate low- $T$  limits deduced from magnetization [5] and NMR [19] data.

cay,  $C_m(t) = C_{eq} + (C_0 - C_{eq}) \exp(-t/\tau_e)$  putting  $t = \tau_e$ , where  $C_{eq}$  is the calculated equilibrium  $C$  of the electron spins (see Refs. [6, 11] for details). As shown in Fig. 3, the rates obtained by these two methods overlap, giving  $\tilde{c} = 0.05 k_B$ . Deducing  $\Gamma$  in this manner is however restricted to  $T$  regions for which the measured  $C_m$  is sufficiently large compared to  $C_0$  and to the nuclear contributions  $C_{hf}$ . Unfortunately, this is not the case for standard  $\text{Fe}_8$  below 1 K.

Figure 3 shows  $\Gamma(T)$  estimated as above together with data obtained at higher temperatures from Ref. [6]. Above 1 K,  $\Gamma$  follows an Arrhenius law that is approximately the same for both  $\text{Fe}_8$  derivatives and corresponds to a thermally activated relaxation over a barrier  $U \approx 22.5$  K. By contrast for  $T < 1$  K, the decrease of  $\Gamma$  of  $^{57}\text{Fe}_8$  abruptly slows down and thus  $\Gamma$  becomes orders of magnitude faster than predicted for activated behavior. Although we cannot extract  $\Gamma$  directly from the low- $T$   $C$  of standard  $\text{Fe}_8$ , we can still estimate an upper bound for it. Using the experimental  $\tau_e(T)$  of standard  $\text{Fe}_8$  and assuming  $\Gamma(T)$  of  $\text{Fe}_8$  to be directly proportional to  $\Gamma(T)$  of  $^{57}\text{Fe}_8$ , we calculate  $C_m(T)$  with either the model of Ref. [16] or exponential decay (see above). The so-obtained  $C_m(T)$  reproduces well the experimental  $C_m(T)$  of standard  $\text{Fe}_8$  if  $\Gamma(T)$  is taken a factor of 3 smaller than that of  $^{57}\text{Fe}_8$ . The same factor was obtained from time-dependent magnetization experiments [5], which provided as well a similar low- $T$  limit of  $\Gamma$ , also plotted in Fig. 3. These data have been successfully interpreted in terms of the PS model, i.e. nuclear spin-mediated tunneling events at a tunneling rate  $1/\tau_t$ , followed by square-root relaxation through redistribution of dipolar fields throughout the sample in combination with addi-

tional spin-flips. In the PS model the tunneling rate is given by  $1/\tau_t \approx \Delta_t^2/E_w$ . With  $\Delta_t \approx 5 \times 10^{-8}$  K and tunneling window  $E_w \approx 0.03$  K, as found for  $^{57}\text{Fe}_8$  [5], one obtains  $1/\tau_t \approx 1 \times 10^{-3} \text{ s}^{-1}$ . The square root relaxation rate is basically given by [17]:  $1/\tau_Q \sim (1/\tau_t)(E_w/E_{dip})^2$ . With  $E_w \approx 0.03$  K and  $E_{dip} \approx 0.1$  K, it follows that  $\tau_Q/\tau_t \approx 10$ , in agreement with the experimental magnetisation relaxation rate of  $10^{-4} \text{ s}^{-1}$  observed at lowest  $T$  [5]. As argued by Morello *et al.* [18] and Baek *et al.* [19], the quantum tunneling fluctuations of the cluster spins should set a  $T$ -independent lower limit to the longitudinal nuclear relaxation rate  $1/T_1^n$  equal to the quantum tunneling rate. Indeed, the calculated value of  $1/\tau_t$  is precisely that attained below about 0.5 K by the experimental  $1/T_1^n$  for  $^{57}\text{Fe}_8$  [19] (Fig. 3).

Our specific heat data thus neatly confirm the isotope effect predicted by the nuclear spin-mediated tunneling (PS) model and previously seen in Ref. [5], but in addition provide strong evidence that in these incoherent quantum tunneling processes an efficient coupling to the phonons has to be involved, i.e. relaxation of the cluster spins is actually to the lattice at a rate corresponding to the square root relaxation, and not towards the nuclear spin-bath, as assumed in the PS model. However, the problem is that, due to the strong average dipolar bias  $E_{dip} \approx 0.1$  K, combined with the very small  $1/\tau_t \approx 1 \times 10^{-3} \text{ s}^{-1}$ , a direct coupling of the tunneling levels to the phonons via the usual spin-lattice interaction by phonon modulation of the crystal field leads to astronomically long relaxation times (inset of Fig. 2). We thus propose a two-step relaxation process as an alternative. All data show that in zero field, in order to flip the spin, we have to rely on the dynamic hyperfine interaction. Through intercluster nuclear spin diffusion [18] the hyperfine bias can fluctuate over an appreciable part of the hyperfine split manifold. Since the width of this energy window  $E_w$  is of the same order (0.01 to 0.1 K) as the dipolar bias, near-resonant conditions for the tunneling levels can be met by the combined action of both biases. Importantly, (i) when the spin flips, both the hyperfine field and the dipolar bias acting on it change sign, implying that in this process energy can be interchanged between nuclear spins and electron dipolar interaction reservoir, and (ii) the reversal of this dipolar bias is instantaneous (picosec) compared to all relevant time scales and produces a temporary disturbance in the local dipolar field distribution. But since the cluster spins are on the nodes of a crystal lattice, they are coupled not only by dipolar but also by weak intercluster elastic (van der Waals) forces. Following general arguments on energy and angular momentum conservation [20], this may result in a temporary local lattice instability, similar as in a Franck-Condon type electronic transition associated with light absorption by lattice defect or impurity states in solids [21]. Thus an unbalance of the interchanged hyperfine and dipolar energy quanta can be taken up by the

lattice as potential energy in the form of a local phonon mode, followed by dissipation into thermal phonons and simultaneous outward evolution of the dipolar field distribution from the ‘defect’. The thermalisation of local vibrational modes due to anharmonic processes has been studied by several authors [21, 22] and the associated times are estimated to be of order  $10^3$  to  $10^4$  s at the low temperatures ( $\approx 0.1$  K) considered here [22], faster indeed than the observed spin-lattice relaxation times (determined by the tunneling rate).

The authors are indebted to J.F. Fernández, A. Morello, S.I. Mukhin, P.C.E. Stamp, I.S. Tupitsyn and W. Wernsdorfer for enlightening discussions. This work is part of the research program of the ‘Stichting FOM’ and is partially funded by the EC-RTN network ‘QuEMolNa’ (No. MRTN-CT-2003-504880) and EC-Network of Excellence ‘MAGMANet’ (No. 515767-2). M.E. acknowledges MIUR for FIRB Project No. RBNE01YLKN.

- 
- [1] See, for instance, D. Gatteschi and R. Sessoli, *Angew. Chem. Int. Ed.* **42**, 268 (2003).
  - [2] N.V. Prokof’ev and P.C.E. Stamp, *Phys. Rev. Lett.* **80**, 5794 (1998); *Rep. Prog. Phys.* **63**, 669 (2000).
  - [3] J.F. Fernández and J.J. Alonso, *Phys. Rev. Lett.* **91**, 047202 (2003); I.S. Tupitsyn and P.C.E. Stamp, *ibid.* **92**, 119701 (2004); J.F. Fernández and J.J. Alonso, *ibid.* **92**, 119702 (2004).
  - [4] C. Sangregorio *et al.*, *Phys. Rev. Lett.* **78**, 4645 (1997); T. Ohm, C. Sangregorio and C. Paulsen, *Eur. Phys. J. B* **6**, 195 (1998); W. Wernsdorfer *et al.*, *Phys. Rev. Lett.* **82**, 3903 (1999).
  - [5] W. Wernsdorfer *et al.*, *Phys. Rev. Lett.* **84**, 2965 (2000).
  - [6] F. Luis *et al.*, *Phys. Rev. Lett.* **85**, 4377 (2000); F.L. Mettes, F. Luis, and L.J. de Jongh, *Phys. Rev. B* **64**, 174411 (2001).
  - [7] N.V. Prokof’ev and P.C.E. Stamp, *J. Low Temp. Phys.* **104**, 143 (1996).
  - [8] M. Evangelisti *et al.*, *Phys. Rev. Lett.* **93**, 117202 (2004).
  - [9] P. Politi *et al.*, *Phys. Rev. Lett.* **75**, 537 (1995).
  - [10] The estimated  $\theta_D \simeq 19$  K differs from  $\theta_D \approx 34$  K obtained in Ref. [6] from fits over a smaller  $T$ -range. From  $\theta_D = 19$  K we estimate the sound velocity,  $c_s = 8 \times 10^2$  m/s, which equals that found from the frequency-dependent susceptibility [6].
  - [11] J.F. Fernández, F. Luis, and J. Bartolomé, *Phys. Rev. Lett.* **80**, 5659 (1998); F. Luis, J. Bartolomé, and J.F. Fernández, *Phys. Rev. B* **57**, 505 (1998).
  - [12] J.F. Fernández (unpublished). For the model used, see J.F. Fernández and J.J. Alonso, *Phys. Rev. B* **62**, 53 (2000); *ibid.* **65**, 189901(E) (2002).
  - [13] P.C.E. Stamp and I.S. Tupitsyn, *Phys. Rev. B* **69**, 014401 (2004); *Chem. Phys.* **296**, 281 (2004); I.S. Tupitsyn, cond-mat/0408220.
  - [14] To simulate the effect of intercluster dipolar coupling and hyperfine interactions, we introduced a static  $B_z = 150$  G. For the model used, see [6].
  - [15] W. Wernsdorfer and R. Sessoli, *Science* **284**, 133 (1999).

- [16] J.F. Fernández, Phys. Rev. B **66**, 064423 (2002).
- [17] N.V. Prokof'ev and P.C.E. Stamp, J. Low Temp. Phys. **113**, 1147 (1998).
- [18] A. Morello *et al.*, Phys. Rev. Lett. **93**, 197202 (2004).
- [19] S.H. Baek *et al.*, Phys. Rev. B **71**, 214436 (2005); Y. Furukawa, Y. Hatanaka, K. Kumagai, S.H. Baek, and F. Borsa, AIP Conf. Proc. (accepted).
- [20] E.M. Chudnovsky, Phys. Rev. Lett. **72**, 3433 (1994).
- [21] A.A. Maradudin, in *Solid State Physics*, edited by F. Seitz and D. Turnbull (Academic Press Inc., New York, 1966), Vol. 19, p. 2-134.
- [22] I.B. Levinson, JETP Lett. **37**, 191 (1983); Mol. Cryst. Liq. Cryst. **57**, 23 (1980).